the isotope effects indicate that the decomposing **2** ions are probably of higher energy than the decomposing **3** or **5** ions, the **2** ions are at least as completely scrambled. This supports the previous conclusions that the identity of the CA spectra of **2** and **5** is not a coincidence, and that isomerization of these ions to a common structure (or mixture of structures) is extensive before collision.[9,10]

In energy region IV the proportion of **2** ions undergoing hydrogen loss before isomerization[19] is much higher than for **3** or **5**. The rate of direct H loss from **2** is nearly as high as the isomerization rate. It seems reasonable that hydrogen loss from the cross-conjugated allylic system of **2** should occur no more readily than hydrogen loss from the linear conjugated system of **5** or the benzylic system of **3**. This suggests that **2** isomerizes much less readily than **3** or **5**, and that the mechanism for the scrambling of the hydrogen atoms in **3** and in **5** does not involve initial conversion to **2**.

Experimental Section

All data were obtained with a Hitachi RMU-7 double-focusing mass spectrometer with an accelerating potential of 3.9 kV, ionizing electrons of 70 eV and 100 μA, and inlet and ion source temperatures of 200°. The geometry of the instrument was reversed so that the magnetic sector precedes the electrostatic sector.[20] The products from the decomposition of a mass-analyzed beam of precursor ions occurring in the field-free region after the magnetic field are determined by scanning the potential of the electrostatic sector. Collisional activation spectra are obtained by increasing the pressure in this field-free region with helium until the precursor ion intensity is reduced to 10% of its original value. The abundance ratios reported in Table I are mean values of at least six measurements. The $C_7(H,D)_8\cdot^+$ abundances have been corrected for isobaric contributions from $C_6{}^{13}C(H,D)_7{}^+$ and from $C_7(H,D]_7{}^+$ due to isotopic impurities. CA data for loss of D have been corrected for loss of H_2, but not for the MI contributions. The kinetic energy released during the cleavage of the C–H or C–D bond shows an isotope effect (energies of 0.107 ± 0.008 eV and 0.136 ± 0.008 eV, respectively) leading to different peak widths, so that it was necessary to use peak areas for relative abundance values.[14] Each of the data in Table III represents the mean value of four measurements.

2-Phenyl-d_5-ethan-1,1,2,2-d_4-ol. Toluene-d_8 (Aldrich, 99% ^{2}H) was refluxed with 1 equiv of Br_2. The resulting benzyl-d_7 bromide was distilled *in vacuo*, converted to the Grignard reagent, and carbonated to produce labeled phenylacetic acid. This was exchanged with basic ^2H_2O for 2 hr at 90° to ensure a high deuterium content at the benzylic position.[21] Reduction with $LiAl^2H_4$ in ether followed by hydrolysis with H_2O, yielded the named compound, isotopic composition d_9, 89.2%; d_8, 10.1%; d_7, 0.7%.

2-Phenyl-d_5-ethan-2-d-1-ol. The labeled phenylacetic acid was exchanged at the hydroxyl group with methanol-*O-d* and converted to the α-bromo acid chloride by refluxing with $SOCl_2$ followed by addition of bromine. This was converted to the methyl ester by addition of methanol-*O-d* at 0°, reduced with $LiAlH_4$ in ether and decomposed with H_2O to yield the named compound, isotopic composition d_6, 90.6%; d_5, 8.5%; d_4, 0.9%. Treatment of the unlabeled bromoester under identical conditions gave a product which contained no more than 1% 1-phenylethanol by nmr analysis.

The *O*-d_1 compounds were prepared by D_2O exchange in the mass spectrometer inlet system. Average isotopic purity values $C_6H_5CH_2CH_2OD$, d_1, 91%; $C_6D_5CHDCH_2OD$, d_7, 84%.

Acknowledgments. We are indebted to Dr. T. Wachs and P. F. Bente III for improvements to the mass spectrometer.

---

(19) As much as 6% of the approximately 44% unscrambled **2** ions (Table II) could be due to **2** ions which had isomerized so that the endomethylene group is retained as the methylene group of **5**; about 10% of the H atoms of the methylene group of **5** are lost specifically (Table II). However, this correction reduces the value for H loss before scrambling of **3** to ∼14%.[11b]

(20) T. Wachs, P. F. Bente III, and F. W. McLafferty, *Int. J. Mass Spectrom. Ion Phys.*, **9**, 333 (1972).

(21) J. G. Atkinson, J. J. Csakvary, G. T. Herbert, and R. S. Stuart, *J. Amer. Chem. Soc.*, **90**, 498 (1968).

Crystal and Molecular Structure of a Caged Polycyclic Tetraoxyazaphosphorane, $(PO_4N)(C_6H_5CN)(C_6H_5)(C_6H_9)$

Walter C. Hamilton,[1a] **John S. Ricci, Jr.,**[1a,b] **Fausto Ramirez,**[1c,d]
Louis Kramer,[1c] **and Peter Stern**[1c]

*Contribution from the Chemistry Department, Brookhaven National Laboratory,
Upton, New York 11793, and the Department of Chemistry,
State University of New York at Stony Brook, Stony Brook, New York 11790.*
Received February 20, 1973

Abstract: The reaction of *N*-phenyl-*N′*-benzoyldiimide with 1-phospha-2,8,9-trioxaadamantane gives a caged adamantanoid tetraoxyazaphosphorane. X-Ray crystallographic analysis shows that the molecule has the geometry of a distorted trigonal bipyramid with a five-membered ring in an apico–equatorial skeletal position, the ring oxygen apical and the ring nitrogen equatorial. The main distortions from the ideal D_{3h} skeletal symmetry are: a bending of the C_3–skeletal axis (169.8° angle), a contraction of the diequatorial angle of the adamantanoid moiety (106.2° angle), and a contraction of the apico–equatorial angle of the five-membered ring (83.8° angle).

Certain α,β-unsaturated ketones react with esters of three-coordinate phosphorus to give relatively stable cyclic oxyphosphoranes,[2] **1**. By analogy with a related cyclic pentaoxyphosphorane[3] whose structure is known from X-ray crystallography,[4] the oxyphos-

---

(1) (a) Brookhaven National Laboratory. (b) Send correspondence to this author at the Department of Chemistry, Windham College, Putney, Vermont. (c) State University of New York at Stony Brook. (d) The support of this research by the U. S. Public Health Service Research Grant No. CA-04769 from the National Cancer Institute and by the National Science Foundation Grant No. GP-23018 is gratefully acknowledged.

(2) (a) F. Ramirez, O. P. Madan, and S. R. Heller, *J. Amer. Chem. Soc.*, **87**, 731 (1965); (b) F. Ramirez, J. F. Pilot, O. P. Madan, and C. P. Smith, *ibid.*, **90**, 1275 (1968); (c) F. Ramirez, J. F. Pilot, and C. P. Smith, *Tetrahedron*, **24**, 3735 (1968).

(3) (a) F. Ramirez, *Accounts Chem. Res.*, **1**, 168 (1968); (b) F. Ramirez, *Bull. Soc. Chim. Fr.*, 3491 (1970).

(4) (a) W. C. Hamilton, S. J. LaPlaca, and F. Ramirez, *J. Amer. Chem. Soc.*, **87** 127 (1965); (b) W. C. Hamilton, S. J. LaPlaca, F. Ramirez, and C. P. Smith, *ibid.*, **89**, 2268 (1967); (c) R. D. Spratley, W. C. Hamilton, and J. Ladel, *ibid.*, **89**, 2272 (1967).

Table I. Nmr Data[a] on Some Oxyphosphoranes Derived from the Reaction of Caged Polycyclic and Acyclic Phosphites with Carbonyl Compounds

Oxyphosphorane no.	Phosphite	Carbonyl compd	$\delta^{31}P$, ppm In CH_2Cl_2	$\delta^{31}P$, ppm In $(CF_3)_2CHOH$	^1H τ, ppm	^1H J_{HP}, Hz	Ref
6	1-Phospha-2,8,9-trioxaadamantane	*N*-Phenyl-*N'*-benzoyldiimide	$+56.8^{b}$	+57.1	5.25^{c}	26.0	
3	Trimethyl phosphite	*N*-Phenyl-*N'*-benzoyldiimide	$+56.7^{d}$		6.46^{e}	13.3	
7	1-Phospha-2,8,9-trioxaadamantane	Hexafluoroacetone	$+42.4^{f}$	+44.1	5.00^{g}	28.0	8, 9
9	Trimethyl phosphite	Hexafluoroacetone	$+49.7^{d}$	+48.3	6.30^{e}	13.4	3
8	1-Phospha-2,8,9-trioxaadamantane	Hexafluorobiacetyl	$+41.7^{h}$	+43.5	5.00^{i}	26.0	10
10	Trimethyl phosphite	Hexafluorobiacetyl	$+46.7^{d}$	+47.1	6.30^{e}	14.0	10

[a] All measurements at 25°. ^{31}P chemical shifts from $H_3PO_4 = 0$, determined at 40.5 MHz. ^1H chemical shifts from $(CH_3)_4Si = 10$, determined at 60 MHz in $CDCl_3$ solution. [b] Quartet, $J_{POCH(methine)} = 25$ Hz. [c] The three methine protons of the cyclohexane moiety give one signal (doublet). The methylene protons give an apparent pair of doublets at τ 7.42 and 8.41 ppm. [d] Decet. [e] The nine protons of the three methoxy groups give one signal (doublet). [f] Quartet, $J_{POCH(methine)} = 28$ Hz. [g] The three methine protons give one signal (doublet). The methylene protons give an apparent pair of doublets at τ 7.20 and 8.26 ppm. [h] Quartet, $J_{POCH(methine)} = 26$ Hz. [i] The three methine protons give one signal (doublet). The methylene protons give an apparent pair of doublets at τ 7.19 and 8.16 ppm.

phoranes **1** can be assigned a trigonal bipyramidal structure with the five-membered ring in the apico–equatorial skeletal position and two oxygen ligands in the apical positions. No stable monooxyphosphorane can be obtained from reactions of the unsaturated ketones with phosphines, R_3P.

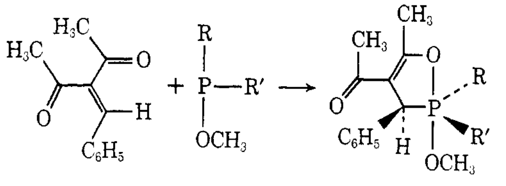

1

$R = R' = OCH_3$
$R = OCH_3$; $R' = C_6H_5$
$R = R' = C_6H_5$

An analogous reaction has been observed[5] with certain *N*-acylimines and trialkyl phosphites; the product now is the cyclic tetraoxyalkylphosphorane, **2**.

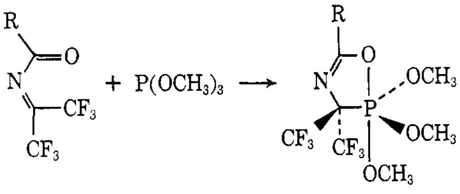

2

We have discovered that *N*-aryl-*N'*-aroyldiimides[6] function effectively in this condensation reaction and give a new type of cyclic tetraoxyazaphosphorane, **3**. This paper describes the synthesis of two of these phosphoranes and the determination of the crystal and molecular structure of one of them by X-ray crystallography.

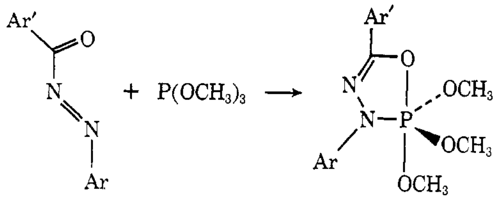

3

Experimental Section

Reaction of *N*-Phenyl-*N'*-benzoyldiimide (4) with 1-Phospha-2,8,9-trioxaadamantane (5). A solution of the phosphite[7–10] (0.8 g) in methylene chloride (3 ml) was added to a stirred solution of the azo compound[6] (1.05 g; 1 mol equiv) in a mixture of methylene chloride (1.5 ml) and hexane (6 ml), at 20°, under N_2. The red solution was stirred 24 hr at 20°, and the tan solid which separated was filtered, washed with hexane (3 ml), and dried at 20° (20 mm). This material (1.80 g) sintered at *ca.* 140° and melted with decomposition at 185–188°. It was the caged oxyphosphorane **6** contaminated with *ca.* 3% of the phosphate ester derived from the oxidation of the phosphite **5**.

The sample of **6** used for elemental and X-ray crystallographic analyses was prepared as follows. A mixture of **6** (1.05 g), carbon tetrachloride (3.5 ml), chloroform (2.5 ml), and methylene chloride (5 ml) was brought to the boiling point, filtered, and evaporated in a slow current of N_2 until crystals of the phosphate impurity appeared. After 1 hr at 0°, the phosphate was filtered off, and the filtrate was again evaported under a slow N_2 current until crystals of the oxyphosphorane **6** appeared. The latter were filtered, washed with carbon tetrachloride, and dried at 20° (20 mm). The colorless crystals of **6** sintered at 150° and melted with decomposition at 189–191°. The nmr data were given in Table I.

Anal. Calcd for $C_{19}H_{19}O_4N_2P$: C, 61.6; H, 5.2; P, 8.3. Found: C, 61.8; H, 5.2; P, 8.2.

The analogous reaction of *N*-phenyl-*N'*-benzoyldiimide with trimethyl phosphite gave an oily oxyphosphorane **3**, Ar = Ar' = C_6H_5, which so far has failed to crystallize; the nmr data on **3** are included in Table I.

Crystal Data. Compound **6**: $C_{19}H_{19}N_2O_4P$; orthorhombic; $Pna2_1$; $a = 12.258$ (2), $b = 9.334$ (1), $c = 15.265$ (2) Å, ($\lambda_{Mo\ K\alpha_1} = 0.7093$ Å) at 21 °C, $Z = 4$; $D_x = 1.36$ g cm^{-3}; D_m (by flotation in aqueous zinc chloride) = 1.30 (2) g cm^{-3}; μ(Mo Kα) = 1.85 cm^{-1}.

Data Collection and Structure Refinement. Precession and Weissenberg photographs of the ($h0l$), ($h1l$), ($hk0$), and ($hk1$) zones showed systematic absences ($0kl$) for $k + l$ odd and ($h0l$) for h odd implying possible space groups $D_{2h}^{7} = Pnma$ or $C_{2v}^{9} = Pna2_1$.

---

(5) (a) K. Burger, J. Fehn, and E. Moll, *Chem. Ber.*, **104**, 1826 (1971); (b) K. Burger and J. Fehn, *Angew. Chem.*, **83**, 761, 762 (1971); (c) *ibid.*, **84**, 35 (1972).

(6) S. G. Cohen and J. Nicholson, *J. Org. Chem.*, **30**, 1162 (1965).

(7) (a) J. G. Verkade and R. W. King, *Inorg. Chem.*, **1**, 948 (1962); (b) J. G. Verkade, R. W. King, and C. W. Heitsch, *ibid.*, **3**, 884 (1964); (c) J. G. Verkade, T. J. Huttemann, M. K. Fung, and R. W. King, *ibid.*, **4**, 83 (1965).

(8) F. Ramirez, S. Pfohl, E. A. Tsolis, J. F. Pilot, C. P. Smith, I. Ugi, D. Marquarding, P. Gillespie, and P. Hoffman, *Phosphorus*, **1**, 1 (1971).

(9) (a) I. Ugi, F. Ramirez, D. Marquarding, H. Klusacek, and P. Gillespie, *Accounts Chem. Res.*, **4**, 288 (1971); (b) I. Ugi and F. Ramirez, *Chem. Brit.*, **8**, 198 (1972).

(10) F. Ramirez, J. Maracek, I. Ugi, and P. Gillespie, *Phosphorus*, in press.

Table II. Positional and Thermal Parameters (× 10^4) for Nonhydrogen Atoms[a,b]

Atom	X	Y	Z	U_{11}	U_{22}	U_{33}	U_{12}	U_{13}	U_{23}
P	2300 (1)	901 (1)	1370	392 (8)	252 (7)	332 (7)	39 (7)	19 (9)	3 (7)
O(1)	1434 (4)	1262 (5)	616 (3)	496 (31)	442 (26)	420 (25)	75 (22)	56 (23)	56 (20)
O(2)	3017 (4)	−253 (5)	816 (3)	747 (36)	409 (27)	366 (24)	107 (24)	141 (26)	57 (20)
O(3)	3158 (8)	2184 (4)	1374 (4)	544 (27)	409 (24)	518 (24)	−146 (19)	67 (30)	−69 (26)
O(4)	1462 (4)	1882 (4)	2082 (3)	484 (28)	308 (21)	460 (25)	143 (21)	99 (23)	13 (21)
N(1)	2244 (4)	−340 (5)	2158 (4)	479 (32)	257 (26)	409 (29)	56 (25)	37 (27)	8 (22)
N(2)	1653 (4)	−63 (5)	2919 (3)	423 (33)	236 (24)	361 (27)	68 (25)	79 (26)	−43 (20)
C(1)	1900 (6)	1726 (8)	−225 (4)	604 (47)	633 (45)	347 (34)	205 (38)	−4 (37)	88 (32)
C(2)	2541 (6)	534 (8)	−631 (5)	577 (51)	558 (41)	509 (45)	−86 (37)	89 (40)	−52 (34)
C(3)	3466 (6)	130 (7)	−30 (5)	649 (51)	438 (37)	437 (38)	185 (38)	30 (39)	−33 (31)
C(4)	4233 (6)	1405 (9)	113 (6)	442 (51)	815 (55)	611 (44)	−62 (43)	144 (41)	−138 (39)
C(5)	3588 (8)	2602 (8)	499 (5)	937 (68)	674 (94)	455 (41)	−352 (50)	57 (47)	−26 (40)
C(6)	2605 (7)	3029 (8)	−68 (5)	1080 (71)	438 (39)	481 (46)	54 (45)	274 (52)	189 (33)
C(7)	527 (5)	1882 (5)	3467 (6)	262 (34)	213 (27)	460 (35)	2 (26)	−26 (29)	−33 (26)
C(8)	−178 (6)	2929 (6)	3230 (4)	515 (42)	423 (35)	397 (32)	36 (34)	−40 (34)	−23 (28)
C(9)	−927 (6)	3527 (7)	3817 (5)	429 (43)	432 (38)	710 (46)	140 (34)	1 (41)	−229 (33)
C(10)	−961 (6)	3015 (8)	4648 (5)	443 (41)	582 (43)	424 (40)	−73 (36)	125 (36)	−117 (34)
C(11)	−226 (6)	1921 (7)	4917 (5)	764 (52)	434 (36)	387 (39)	59 (39)	103 (42)	101 (32)
C(12)	488 (5)	1361 (6)	4310 (5)	429 (43)	305 (31)	580 (46)	61 (30)	49 (37)	9 (29)
C(13)	2782 (5)	−1778 (6)	2149 (4)	447 (38)	308 (32)	317 (31)	141 (30)	105 (32)	−29 (26)
C(14)	3750 (5)	−2019 (7)	2402 (5)	436 (48)	440 (16)	634 (42)	88 (31)	14 (39)	88 (31)
C(15)	4142 (7)	−3419 (8)	2446 (5)	592 (50)	519 (41)	564 (49)	263 (41)	111 (41)	124 (37)
C(16)	3485 (7)	−4550 (7)	2207 (5)	862 (61)	334 (33)	586 (44)	208 (39)	36 (49)	47 (32)
C(17)	2412 (7)	−4310 (7)	1948 (5)	976 (65)	300 (37)	500 (41)	123 (38)	−12 (43)	−90 (31)
C(18)	2010 (6)	−2888 (7)	1936 (4)	555 (43)	338 (35)	456 (37)	30 (32)	−131 (37)	−96 (29)
C(19)	1254 (5)	1204 (6)	2816 (4)	345 (39)	319 (33)	332 (30)	−6 (27)	−74 (29)	−2 (24)

[a] The form of the anisotropic thermal ellipsoid is $\exp[-2\pi^2\Sigma_{ij}a_i{}^*a_j{}^*U_{ij}h_ih_j]$. [b] Numbers in parentheses here and in succeeding tables are estimated standard deviations in the least significant digits.

The latter was confirmed by the structure solution and refinement. The cell dimensions were determined by a least-squares fit of the observed 2θ angles for 29 reflections centered automatically on a four-circle diffractometer.

Intensity data were collected from a colorless crystal of approximate hexagonal prismatic habit and dimensions 0.1 × 0.05 × 0.2 mm. Data were obtained on a computer-controlled Picker four-circle diffractometer[11] using Mo Kα radiation monochromatized by reflection from the (002) plane of a highly oriented pyrolytic graphite monochromator. Two independent sets of data ($\bar{h}kl$ and $\bar{h}\bar{k}\bar{l}$) were collected for 2σ(Mo Kα) < 50°. The 3000 reflections were averaged to give 1135 independent reflections with $F_o{}^2 > 3\sigma_{\text{count}}(F_o{}^2)$ with $\sigma(F_o{}^2)$ being based on Poisson counting statistics. The intensities of two standard reflections were measured periodically, and there was no evidence of crystal deterioration. Data were collected by θ–2θ step scans using a scan width $\Delta 2\theta = 1.80\ (1 + \tan\theta)$ and a step size $\delta 2\theta$ of 0.02°. The center of the scan range was set at the Bragg angle calculated for 0.7104 Å. Background was measured as the average of the first and last five points of the scan. The take-off angle was 2.2°, and a pulse height–pulse shape discrimination system was used.

Structure factors were derived in the usual way; no absorption correction was necessary. Normalized structure factors (E's) were used in a multiple-solution direct methods technique as described by Germain, Main, and Woolfson[12] to determine phases from which an E map revealed the coordinates of about half the nonhydrogen atoms. The remaining atoms were located by a series of Fourier and structure factor calculations. The structure was refined by full-matrix least squares, minimizing the function $\Sigma w\Delta^2$ with $\Delta = |F_o| - |F_c|$ and weights $w = 4F_o{}^2/\sigma^2(F_o{}^2)$ and $\sigma^2(F_o{}^2) = \sigma^2{}_{\text{count}}(F_o{}^2) + (0.04F^2)^2$. The atomic scattering factors for all nonhydrogen atoms were taken from a standard source,[13] while that for the hydrogen atoms (all located in a difference map following an isotropic refinement) was the best spherically averaged value of Stewart, *et al.*[14]

The final least-squares cycles included anisotropic thermal parameters for the nonhydrogen atoms; the hydrogen atom positions were fixed in idealized locations with fixed bond lengths of 0.98 Å and an isotropic thermal parameter $B = 5.5$ Å^2. The final values of $R_1 = \Sigma||F_o| - |F_c||/\Sigma|F_o|$ and $R_2 = [[\Sigma w||F_o| - |F_c||^2]/\Sigma wF_o{}^2]^{1/2}$ were 0.049 and 0.052, respectively,[15] and $[\Sigma w||F_o| - |F_c||^2]^{1/2}$ was 2.22. The maximum density in a final difference electron density synthesis was 0.34 electrons Å^{-3}, approximately 10% of the height of a carbon atom. The final parameters are presented in Tables II and III and the structure amplitudes as $10|F_o|$ and $10|F_c|$ in Table IV.[16]

Table III. Calculated Hydrogen Atom Positions (× 10^4)[a]

Atom	X	Y	Z
H-1	1327	2026	−640
H-3	3862	−676	−292
H-5	4097	3413	562
H-2-1	2830	823	−1207
H-2-2	2055	−304	−720
H-4-1	4550	1695	−460
H-4-2	4840	1112	498
H-6-1	2874	3390	−640
H-6-2	2183	3773	218
H-8	−132	3345	2617
H-9	−1428	4316	3630
H-10	−1467	3421	5088
H-11	−286	1531	5518
H-12	993	582	4488
H-14	4229	−1196	2568
H-15	4898	−3636	2636
H-16	3777	−5536	2239
H-17	1964	−5149	1784
H-18	1258	−2695	1747

[a] Hydrogen atom H-1 is attached to carbon C-1. All were assigned a B of 5.5 Å^2 in the structure factor calculation.

Discussion of Results

Reaction of *N*-Phenyl-*N*′-benzoyldiimide (4) with Phosphite Esters. The X-ray data, which will be dis-

---

(11) D. R. Beaucage, M. A. Kelly, D. Ophir, S. Rankowitz, R. J. Spinrad, and R. van Norton, *Nucl. Instrum. Methods*, 40 26 (1966).

(12) G. Germain, P. Main, and M. M. Woolfson, *Acta Crystallogr., Sect. B*, 26, 274 (1970); *Acta Crystallogr., Sect. A*, 27, 368 (1971).

(13) "International Tables for X-ray Crystallography," Vol. 3, Kynoch Press, Birmingham, England, 1962, Table 3.3.1A.

(14) R. F. Stewart, F. R. Davidson, and W. T. Simpson, *J. Chem. Phys.*, 42, 3175 (1965).

(15) These values were 0.099 and 0.119 before addition of hydrogen atoms and anisotropic refinement.

(16) See paragraph at end of paper regarding supplementary material.

Table V. Bond Distances (Å) and Angles (deg)

		In Trigonal Bipyramid			
P–O(2)	1.627 (5)	O(2)–P–O(4)	169.8 (2)	O(4)–P–O(3)	89.4 (2)
P–O(4)	1.754 (4)	O(2)–P–O(3)	98.4 (2)	O(4)–P–O(1)	87.0 (2)
P–O(1)	1.601 (5)	O(2)–P–O(1)	97.1 (3)	O(1)–P–O(3)	106.3 (2)
P–O(3)	1.590 (4)	O(2)–P–N(1)	86.4 (2)	O(1)–P–N(1)	129.5 (3)
P–N(1)	1.671 (5)	O(4)–P–N(1)	83.8 (2)	O(3)–P–N(1)	123.1 (3)
		In Adamantanoid Portion			
O(1)–C(1)	1.471 (8)	P–O(1)–C(1)	115.6 (4)	C(3)–C(4)–C(5)	108.1 (6)
O(2)–C(3)	1.448 (8)	P–O(3)–C(5)	115.3 (4)	O(3)–C(5)–C(4)	110.3 (6)
O(3)–C(5)	1.488 (9)	P–O(2)–C(3)	120.3 (4)	O(3)–C(5)–C(6)	107.3 (6)
C(1)–C(2)	1.496 (10)	O(1)–C(1)–C(2)	110.3 (6)	C(4)–C(5)–C(6)	112.9 (6)
C(2)–C(3)	1.506 (10)	O(1)–C(1)–C(6)	108.7 (6)	C(1)–C(6)–C(5)	109.1 (6)
C(3)–C(4)	1.532 (11)	C(2)–C(1)–C(6)	111.4 (6)	Mean O–C–C	108.8 (5)
C(4)–C(5)	1.493 (12)	C(1)–C(2)–C(3)	109.2 (6)	Mean C–C–C	110.2 (7)
C(5)–C(6)	1.532 (12)	O(2)–C(3)–C(2)	108.6 (6)		
C(6)–C(1)	1.511 (11)	O(2)–C(3)–C(4)	107.4 (6)		
Mean C–C	1.512 (7)	C(2)–C(3)–C(4)	110.7 (6)		
		In and Attached to Five-Membered Ring			
N(1)–N(2)	1.394 (7)	P–N(1)–N(2)	119.5 (4)		
N(2)–C(19)	1.289 (7)	P–N(1)–C(13)	128.1 (4)		
C(19)–O(4)	1.311 (7)	N(2)–N(1)–C(13)	112.3		
C(19)–C(7)	1.477 (8)	N(1)–N(2)–C(19)	105.4 (5)		
N(1)–C(13)	1.454 (7)	N(2)–C(19)–O(4)	118.3 (5)		
		N(2)–C(19)–C(7)	122.6 (5)		
		C(7)–C(19)–O(4)	119.0 (5)		
		P–O(4)–C(19)	113.0 (4)		
		Phenyl Groups			
C(7)–C(8)	1.381 (8)	C(19)–C(7)–C(8)	121.1 (5)	N(1)–C(13)–C(18)	117.3 (5)
C(8)–C(9)	1.385 (9)	C(19)–C(7)–C(12)	119.9 (5)	N(1)–C(13)–C(14)	121.0 (6)
C(9)–C(10)	1.356 (10)	C(8)–C(7)–C(12)	118.9 (5)	C(14)–C(13)–C(18)	121.6 (6)
C(10)–C(11)	1.422 (10)	C(7)–C(12)–C(11)	121.1 (6)	C(13)–C(18)–C(17)	119.3 (6)
C(11)–C(12)	1.377 (9)	C(12)–C(11)–C(10)	118.8 (6)	C(18)–C(17)–C(16)	118.8 (6)
C(12)–C(7)	1.377 (8)	C(11)–C(10)–C(9)	120.2 (6)	C(17)–C(16)–C(15)	120.4 (6)
C(13)–C(14)	1.359 (9)	C(10)–C(9)–C(8)	119.5 (6)	C(16)–C(15)–C(14)	120.2 (7)
C(14)–C(15)	1.395 (9)	C(9)–C(8)–C(7)	121.4 (6)	C(15)–C(14)–C(13)	119.7 (7)
C(15)–C(16)	1.377 (10)	Mean C–C–C	120.0 (3)		
C(16)–C(17)	1.393 (10)				
C(17)–C(18)	1.416 (9)				
C(18)–C(13)	1.378 (9)				
Mean C–C	1.385 (5)				

cussed in detail below, provide a firm basis for the assignment of a structure with pentacovalent phosphorus,[17] **6**, to the 1:1 adduct made from *N*-phenyl-*N'*-benzoyldiimide (**4**) and the adamantanoid phosphite **5**. The similarity in the ^{31}P chemical shifts of **6**, and of its trimethyl phosphite analog **3** (Ar = Ar' = C_6H_5), leaves no doubt concerning the pentacovalent character of the phosphorus in the latter also.

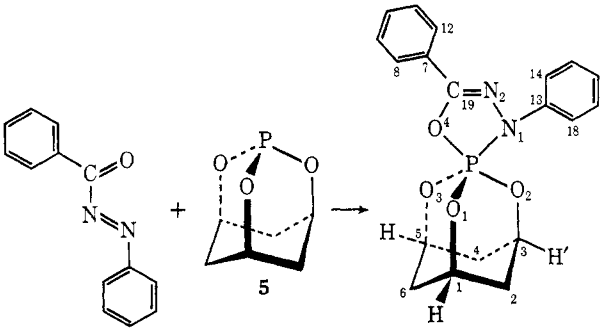

4 5 6

The results of this investigation strengthen considerably the structural assignments **7** and **8** for the products of the reaction of the adamantanoid phosphite **5** with 2 mol of hexafluoroacetone,[8,9,18,19] CF_3COCF_3, and with 1 mol of hexafluorobiacetyl,[10] $CF_3COCOCF_3$, respectively. Note in Table I the consistent values of the ^{31}P chemical shifts and the similarities in the shifts and in the coupling constants of the methine protons of the cyclohexane moiety in the three-caged polycyclic oxyphosphoranes.

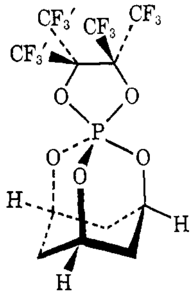

7

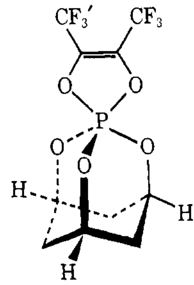

8

It is also evident that the corresponding products **9** and **10** derived from trimethyl phosphite belong to the same family of oxyphosphoranes.

---

(17) The numbering of the atoms in **6** corresponds to that used in the X-ray crystallographic analysis, see Figure 1. **6** is based on an ideal trigonal bipyramidal skeleton with D_{3h} symmetry. The actual deviations from this skeletal symmetry will be discussed below.

(18) (a) P. Gillespie, P. Hoffman, H. Klusacek, D. Marquarding, S. Pfohl, F. Ramirez, E. A. Tsolis, and I. Ugi, *Angew. Chem., Int. Ed. Engl.*, **10**, 687 (1971); (b) *ibid.*, **10**, 712 (1971), footnote*; (c) *ibid.*, **10**, 702 (1971).

(19) (a) F. Ramirez and I. Ugi, *Advan. Phys. Org. Chem.*, **9**, (1971); (b) *ibid.*, **9**, 80 (1971); (c) *ibid.*, **9**, 60 (1971).

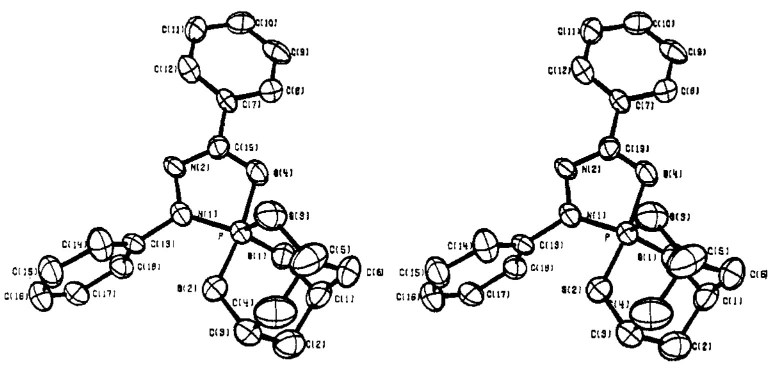

Figure 1. A stereoscopic drawing of an isolated molecule of $C_{19}H_{19}N_2O_4P$. The 50% probability vibrational ellipsoids are shown.

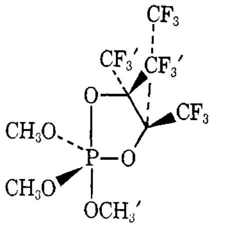

9

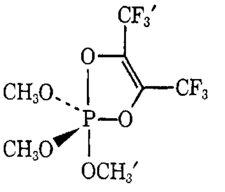

10

Table I discloses other interesting characteristics of the phosphoranes. (1) The ^{31}P nmr shifts are insensitive to the nature of the solvent, including the relatively acidic hexafluoroisopropyl alcohol. This is presumptive evidence against the existence in solution of equilibria involving the five-coordinate covalent and the ion-pair forms of the phosphoranes. (2) The two adamantanoid pentaoxyphosphoranes **7** and **8** have slightly less shielded ^{31}P nuclei than the corresponding monocyclic analogs **9** and **10** ($\Delta\delta \sim$ 5–7 ppm). This slight effect of the adamantanoid cage on the ^{31}P shift is, however, unnoticeable in the tetraoxyazaphosphoranes **6** and **7**. (3) The relatively large coupling of the methine protons with the phosphorus (*ca.* 27 Hz) is attributable to the nature of the dihedral angle formed by the planes which contain P–O–C and O–C–H. The data in Table I will be discussed further in the section dealing with the dynamic stereochemistry of the phosphoranes.

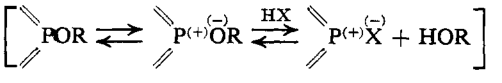

Molecular Structure. The relevant interatomic distances, bond angles, and their standard deviations are summarized in Table V and were calculated from the positional parameters in Tables II and III and the correlation matrix. The least-square planes are given in Table VI. The structure will be discussed with reference to Figure 1, which shows the numbering system for the atoms in the molecule and also the vibrational thermal ellipsoids for the atoms. Formula **6**, based on an idealized D_{3h} skeletal symmetry, serves to emphasize the deviations of the actual molecule from ideality. This deviation is mainly reflected in the values of the following angles: O(4)–P–O(2) = 169.8°; O(4)–P–N(1) = 83.8°; N(1)–P–O(12) = 86.4°; O(1)–P–O(2) = 97.1°; O(3)–P–O(2) = 98.4°; O(1)–P–O(3) = 106.2°; and O(1)–P–N(1) = 129.5°. Conversely, one could say that the preferred trigonal bipyramidal geometry of five-coordinate phosphorus is imposing itself upon the constraints of the adamantanoid ring system, as shown by the "opening" of the angle O(1)–P–O(3) toward 120° and the "closing" of the angles O(3)–P–O(2) and O(1)–P–O(2) toward smaller values.

Table VI. Weighted Least-Squares Planes[a]

1. P,N(1),O(1),O(3)
$0.5633X - 0.5620Y - 0.6056Z = -0.1658$; P, 0.01; N(1), −0.10; O(1), −0.08; O(3), −0.07
2. P,O(4),N(1),O(2)
$-0.8226X - 0.3840Y - 0.4195Z = -3.5143$; P, −0.00; O(4), 0.03; N(1), −0.01; O(2), 0.04
3. P,N(1),N(2),C(19),O(4)
$-0.8124X - 0.3995Y - 0.4247Z = -3.5139$; P, −0.00; N(1), 0.01; N(2), −0.00; C(19), −0.01; O(4), 0.01
4. P,N(1),N(2),C(19),O(4),C(7),C(13)
$-0.8148X - 0.3858Y - 0.4327Z = -3.4258$; P, −0.00; N(1), −0.02; N(2), −0.03; C(19), −0.02; O(4), 0.01; C(7), 0.03; C(13), 0.05
5. C(7),C(8),C(9),C(10),C(11),C(12)
$-0.6746X - 0.6838Y - 0.2780Z = -3.1097$; C(7), 0.00; C(8), −0.01; C(9), 0.01; C(10), 0.01; C(11), −0.02; C(12), 0.01
6. C(13),C(14),C(15),C(16),C(17),C(18)
$0.2984X + 0.0791Y - 0.9512Z = -2.2713$; C(13), 0.01; C(14), 0.01; C(15), −0.02; C(16), 0.01; C(17), 0.01; C(18), −0.02
7. P,O(4),C(19),N(2),N(1),O(2)
$-0.8216X - 0.3844Y - 0.4210Z = -3.5150$; P, 0.00; O(4), 0.03; C(19), 0.01; N(2), −0.00; N(1), −0.01; O(2), 0.04

Angles between Planes A and B

Plane A	Plane B	Angle, deg	Plane A	Plane B	Angle, deg
1	2	89.63	3	4	0.92
1	3	88.62	3	5	20.06
1	4	88.86	3	6	82.53
1	5	80.06	3	7	1.03
1	6	45.60	4	5	20.96
1	7	89.53			
2	3	1.10	4	6	82.07
2	4	0.88	4	7	0.78
2	5	20.92	5	6	89.48
2	6	82.92	5	7	20.91
2	7	0.11	6	7	82.83

[a] *X*, *Y*, and *Z* are in orthogonal coordinates with deviations of the individual atoms from the planes given in Å.

The five-membered ring is a highly distorted pentagon which contains angles ranging from O(4)–P–N(1) = 83.8° to P–N(1)–N(2) = 119.5°. The cyclohexane ring has the classical chair form with C–C–C–C torsion angles 58, −62, 58, −55, 57, and −55° and a

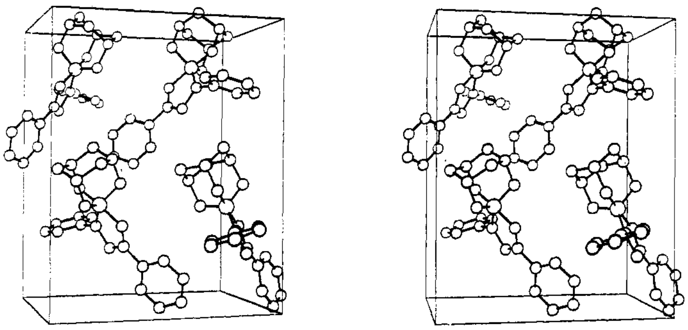

Figure 2. A stereoscopic drawing of four molecules of $C_{19}H_{19}N_2O_4P$ whose central phosphorus atoms all lie within the same unit cell. View approximately along *b*, and *c* is vertical.

mean C–C bond length of 1.512 (7) Å. The C–C–C bond angle is 111.7 (6)° at the carbon atoms, where oxygen is attached, and 108.8 (4)° at the other carbons. One phenyl group is nearly coplanar with the planar five-membered ring (torsion angle O(4)–C(19)–C(7)–C(8) = 19.8°) while the other is nearly orthogonal (N(2)–N(1)–C(13)–C(18) = 77.4°). The phenyl groups have normal geometry.

The five-membered ring occupies an apico–equatorial position, as was the case in another five-membered cyclic oxyphosphorane.[4] The apical bonds are longer than the corresponding equatorial bonds, which is typical of trigonal bipyramidal phosphorus. As would be expected from electronegativity considerations, the ring oxygen is apical and the ring nitrogen is equatorial.

The unit cell contents are shown in Figure 2. There are no unusually short intermolecular contacts.

Static and Dynamic Stereochemistry of Caged Polycyclic Oxyphosphoranes. The results of this investigation and previous data obtained in these laboratories[2,3,8-10,18,19] provide an opportunity to contrast the stereochemistry of the caged polycyclic oxyphosphoranes in the crystal and in solutions.

The nmr data summarized in Table I pertain to solutions at ambient temperature. In all cases the three methine protons of the cyclohexane moiety in the caged phosphoranes give rise to one signal. Likewise, the nine protons of the three methoxy groups in the monocyclic phosphoranes produce one resonance. The proton spectra of the caged and the monocyclic derivatives of hexafluoroacetone and of hexafluorobiacetyl, **7–10**, have been studied in $CDCl_3$ solution down to about −50°, without evidence of significant changes. In one case, **7**, the proton spectrum was followed to −100° in 3:1 SO_2–CF_2Cl_2 without significant changes.

At ambient temperature, the ^{19}F nmr spectra of **7–10** exhibit only one signal in methylene chloride solutions. The ^{19}F spectrum of **7** could be followed[20] down to −165° in the solvent mixture 70% vinyl chloride and 30% fluorodichloromethane; the results show that the coalescence temperature in this case must be below this temperature and that the energy barrier for the exchange of the ligands among the skeletal positions must be quite low, <5 kcal/mol.[21] The ^{13}CFT nmr[20] of **7** in methylene chloride solution at room temperature, in conjunction with the other data, strongly support the view that **7** is indeed undergoing relatively rapid permutational isomerization in the range +30 to −165°, in the time scale of the nmr. The data are not as extensive for the other phosphoranes in Table I, but it is reasonable to expect a comparable behavior for the pentaoxyphosphoranes. There is as yet no variable temperature ^1H nmr data for the azaphosphoranes **3** and **6**, although the presence of one nitrogen ligand could result in a significantly higher energy barrier for the isomerization.

The chemical properties of these phosphoranes, and in particular the solvent-insensitivity of the ^{31}P nmr shifts,[3,18,19] suggest that their permutational isomerizations occur by an intramolecular bond-deformation process. A plausible mechanism for such a process, namely the turnstile rotation (TR), was proposed recently.[8,9,18,19] As applied to the isomerization of **6**, this mechanism is shown in Scheme I. The adaman-

Scheme I

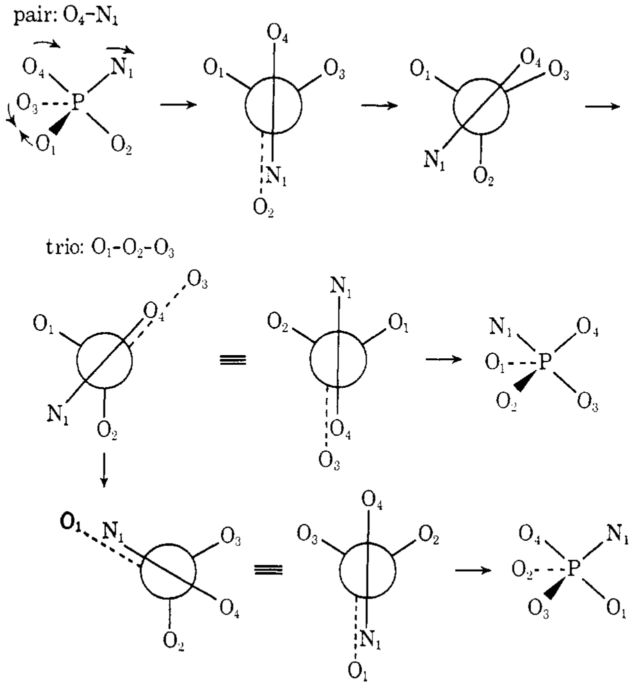

---

(20) F. Ramirez, S. Pfohl, F. Lin, I. Ugi, P. Hoffman, and D. Marquarding, manuscript in preparation.

(21) Earlier studies on the variable temperature ^1H and ^{19}F nmr spectra of the adamantanoid-hexafluoroacetone phosphorane **7** established the occurrence of relatively rapid permutational isomerization to at least −100°. However, due to difficulties stemming from lack of solubility of **7** in suitable nmr solvents, those studies led to the erroneous conclusion that signal coalescence occurred at approximately −120° (ref 18b and 19b).

tanoid moiety functions as the "trio" and the five-membered ring functions as the "pair" in the TR. The diequatorial angle of the trio contracts from 120 to about 90°, while the pair tilts approximately 9° toward the apical ligand of the trio. Simultaneously, there is an internal rotation of the pair relative to the trio as illustrated by means of Newman projections. The rotation reaches 30° at the barrier configuration and 60° at the completion of the TR. Past the barrier configuration there is a simultaneous tilt of the pair away from the ligand that will become apical in the new trigonal bipramid and also an expansion of the angle that will become the new diequatorial angle (*ca.* 90° → 120°). After a single TR, the new isomer has an apical nitrogen; however, depending on energetic considerations, it is entirely possible that this new trigonal bipyramid is never reestablished. This could come about if the internal rotation of pair *vs.* trio continues toward an overall value of 120° (double TR), in which case the new trigonal bipyramid retains the apical placement of the oxygen of the five-membered ring, while the ligands of the adamantanoid moiety exchange relative positions following the apparent motions of a "turnstile."

In the adamantanoid phosphoranes the nearly trigonal bipyramidal arrangement of the phosphorus valencies can be achieved only as a result of a certain amount of distortion of the cage which requires some energy. This energy is released as the bipyramid goes over into the 30°-TR barrier configuration where the adamantanoid moiety possesses C_{3v} local symmetry. The combination of a relatively energetic distorted trigonal bipyramid and a favorable 30°-TR barrier could explain the remarkably low barrier for the positional exchange of the ligands in these highly constrained caged phosphoranes.

Calculations of the binding energies of various configurations of the PF_5 molecule, made by the CNDO/2 approximation to the MO-LCAO method, showed[18,19] that the most stable 30°-TR barrier configuration model has one 85° F-P-F angle in the pair and three 95° F-P-F angles in the trio. It may, therefore, be significant that the molecule of the caged phosphorane **6** in the crystal has an 83.8° O(4)-P-N(1) angle (the pair) and a set of three angles: 97.1° O(1)-P-O(2), 98.4° O(3)-P-O(2), and 106.2° O(1)-P-O(3) (the trio). The first two angles of this set represent expansions of the 90° apico-equatorial angles, while the third angle corresponds to a significant contraction (*ca.* −14°) of the ideal 120° diequatorial angle. In fact, to reach the 30°-TR barrier, this molecule needs only some relatively minor adjustments.

Finally, in the TR process the pair tilts toward the apical ligand of the trio by approximately 9° and, in fact, one finds that the O(4)-P-O(2) angle in **6** is 169.8° rather than the ideal 180°. In summary, the deviations from tne ideal D_{3h} skeletal symmetry found in the molecule of **6** in the crystals are in the direction required for the operation of the turnstile rotation mechanism in the solution of the compound.

Supplementary Material Available. Table IV will appear following these pages in the microfilm edition of this volume of the journal. Photocopies of the supplementary material from this paper only or microfiche (105 × 148 mm, 20 × reduction, negatives) containing all of the supplementary material for the papers in this issue may be obtained from the Journals Department, American Chemical Society, 1155 16th St., N.W., Washington, D. C. 20036. Remit check or money order for $3.00 for photocopy or $2.00 for microfiche, referring to code number JACS-73-6335